


Cite this: *RSC Adv.*, 2020, 10, 27042

Quantitative determination of leukocyte esterase with a paper-based device†

Mei-Lin Ho,^a Wei-Fang Liu,^a Hsin-Yi Tseng,^a Yu-Tzu Yeh,^a Wei-Ting Tseng,^a Yin-Yu Chou,^a Xin-Ru Huang,^a Hung-Cheng Hsu,^a Li-Ing Ho^{bc} and Sheng-Wei Pan^{id}*^{bc}

The commercially-available colorimetric urine dipstick for the early detection of urinary tract infection (UTI) has several limitations. The quantitative determination of urinary leukocyte esterase (LE) for predicting UTI remains uncertain. This study presents a paper-based analytical device to detect LE (LE-PAD) as a point-of-care quantitative test for UTI. The LE-PAD is composed of a coating of mixed 3-(*N*-tosyl-L-alaninyloxy)-5-phenylpyrrole (PE) and 1-diazo-2-naphthol-4-sulfonic acid (DAS) deposited onto a silver conducting film (Ag film). The LE/urine reacts with the PE and DAS, and the resulting products in turn react with the silver coating, causing a change in resistivity. The quantitative calibration curve was established in this study and has been used to analyse urine samples from inpatients with urinary catheters ($n = 21$). The results revealed that the level of LE determined by LE-PADs was predictive of UTI diagnosis with an area under the receiver operating characteristic curve of 0.875 (95% confidence interval, 0.704–1.000). Using an appropriate cut-off value, the sensitivity and specificity of UTI diagnosis by LE-PAD were 87.5% and 92.3%, while the LE-positivities of urine dipsticks were 62.5% and 76.9%, respectively. For UTI diagnosis, the LE-PAD demonstrated positive and negative likelihood ratios of 11.38 and 0.14, suggesting that the novel LE-PAD is a reliable test.

Received 13th April 2020
Accepted 9th July 2020

DOI: 10.1039/d0ra03306e

rsc.li/rsc-advances

Introduction

Urinary tract infections (UTIs) are a bacteriuria-related infectious disease and are common infections across all age groups, affecting 150 million people each year worldwide.^{1–3} Early detection of UTIs is important in clinical settings because delays in diagnosis and treatment may result in bacteremia and urosepsis. In the United States, the annual cost of UTIs to the health care system is \$ 1.6 billion.⁴

Although urinalysis for pyuria and urine culture for bacteriuria can be used to confirm a diagnosis of UTI, they require hospital-based facilities, and the latter test is time-consuming.^{3,5,6} Other screening diagnostic tests for UTI are available.⁵ For example, urine dipsticks that test for the presence of enzyme leukocyte esterase (LE) and nitrite in the urine are the most used point-of-care tests. However, earlier meta-analyses showed that dipstick results are not very accurate.

The dipsticks provide only limited information in the form of qualitative measurement.⁵ Recently, the search for biomarkers of UTI has attracted attention.^{3,5} To reduce the labour cost of culture tests, more recent studies have used flow cytometry for screening out negative urine samples.⁷ Recently, mass spectrometry has been suggested for bacterial identification, but several issues need to be resolved.^{8,9} Optical NIR-infrared spectroscopy is feasible for non-invasive monitoring of UTI.¹⁰ Other analytical methods, such as the nucleic acid-based method,¹¹ isothermal microcalorimetry¹² and nano-biosensors¹³ have also been utilized to identify bacteria.

LE is an enzyme secreted by neutrophils and is a marker of infection.¹⁴ For example, Li *et al.* used the LE strip test on synovial fluid to establish a diagnosis of periprosthetic joint infection.¹⁵ Sapey *et al.* demonstrated that the LE strip may provide a diagnosis of spontaneous bacterial peritonitis.¹⁶ Although this test is useful for quick assessment of infections, the reported sensitivity varies. Therefore, a new approach to improve the detection of infections is needed. Recently, Hanson *et al.* have synthesized several substrates for LE via amperometric method.^{17,18} The synthesized substrates react with LE in solution, releasing 1,4-hydroquinone, which is then oxidized and yields anodic current in direct proportion to the activity of LE.¹⁷

On the other hand, silver nanoparticle-based inks with distinct electrical, optical and chemical properties have been

^aDepartment of Chemistry, Soochow University, Taipei 111, Taiwan. E-mail: meilin_ho@gm.scu.edu.tw; Fax: +886 2 2881 1053; Tel: +886 2 2881 9471 ext. 6827

^bDepartment of Chest Medicine, Taipei Veterans General Hospital, Taipei 11217, Taiwan. E-mail: swpan2@vghtpe.gov.tw

^cSchool of Medicine, National Yang-Ming University, Taipei 11221, Taiwan

† Electronic supplementary information (ESI) available: EDS spectra, contact angle measurement, UV-vis and IR spectra, storage test of LE-PAD, potential interfere concentrations, data of real sample measurement, and tabulated statistical analysis. See DOI: 10.1039/d0ra03306e



used widely in commercially-derived products.^{19,20} Merilampi *et al.* used silver ink on stretchable substrates and demonstrated a change in resistance during stretching of the materials.²¹ Andersson *et al.* deposited inkjet-printed silver nanoparticles on paper. Resistance change occurred with humidity increases.^{22,23} Kim *et al.* presented inkjet printing of silver nanoparticles on cellulose-based and synthetic Teslin papers for radio frequency identification (RFID)-based sensing.²⁴

The above studies encouraged us to investigate applications based on silver nanoparticle ink. Recent electrochemical method has been proposed and applied it to the detection of various diseases.²⁵ In our previous work, a microfluidic paper-based device developed by chemiresistive method was used for quantitative detection of nitrite with a low detection limit.²⁶

Since UTIs are common, especially in persons with indwelling urinary catheters, clinically-effective and cost-effective tests for diagnosis and investigation are needed.⁴ Regarding the urine dipstick assay, the Kuppusamy group found that the reliability of UTI diagnosis was highest when nitrite, leukocyte and blood were considered together.²⁷ However, for patients with indwelling urinary catheters, who have a high risk for UTI, Schwartz *et al.* reported that the sensitivity of LE and nitrite were as low as 30% and 52%, whereas the combined sensitivity and specificity were 57% and 81%, respectively.²⁸ Here, the sensitivity of a test is its ability to correctly identify patients with a disease, *i.e.* clinical diagnosis of urinary tract infection (UTI).²⁹ The low sensitivity to LE of dipsticks is an obstacle for early detection of UTI.

Therefore, the present study aimed to develop a novel chemiresistive method for quantitative determination of LE. We proposed a paper-based device containing a coating of mixed 3-(*N*-tosyl-L-alaninyloxy)-5-phenylpyrrole (PE) and 1-diazo-2-naphthol-4-sulfonic acid (DAS) as a recognition molecule for reaction with the analyte (LE). Under the PE and DAS coating, a silver film, formed by depositing silver ink on paper substrate and lightly sintering it, functioned as a signal unit for the detection of the signal of the product (azo dye) to react with the silver film (Ag film) (see Scheme 1). The resistance in the sensor increased with higher concentrations of LE. An advantage of

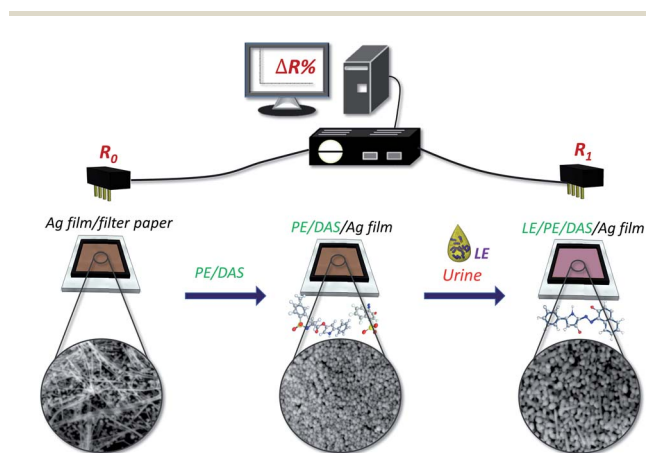
this sensing platform is that it can quantify the content of LE. We used the present electrochemical sensor to analyse urine samples from inpatients with indwelling urinary catheters, and the results were compared with those of the urine dipstick method.

Results and discussion

The design and optimization of the LE-PAD

It is well known that the LE strip provides limited resolution, with only 3–4 degrees of range and low sensitivity to low LE activity.^{15,17} To establish a quantitative method for detecting LE, we improved the qualitative screening method of LE and developed an electrochemical method for the determination of LE in human urine. To examine the potential for silver film to react with LE, the resistance change of silver film (Ag film) in the presence of LE was measured (Fig. 1(A)). When the PE/DAS was coated onto silver film directly (PE/DAS/Ag film), we observed a significant signal increase in the presence of LE, suggesting that the reaction of PE and DAS with LE would increase the change in the signal.

To investigate the optimized silver coating to give a signal change, the difference in initial resistivity (R_0) in response to $8.0 (\times 5.1 \text{ U mg}^{-1} \text{ mL}^{-1})$ LE was examined. As shown in Fig. 1(B), the maximum resistivity change was observed at around $14\text{--}16 \text{ } \Omega \text{ sq}^{-1}$. For the requirement of quantitative analysis, initial resistivity at $16 \text{ } \Omega \text{ sq}^{-1}$ with smaller deviation was chosen. To examine the sensing effect of LE using the optimized conditions of LE-PADs, the effects of the reaction reagent and buffer concentration were subsequently tested. The optimum molar ratio of PE *versus* DAS was investigated and is illustrated in Fig. 1(C). In this test, PE in acetonitrile and DAS in buffer solution were mixed first and dripped onto the Ag film (PE/DAS/Ag film), and then dried in ambient conditions. After the device was dried, $8.0 (\times 5.1 \text{ U mg}^{-1} \text{ mL}^{-1})$ LE was added, and the



Scheme 1 The illustration of LE-PADs for LE detection.

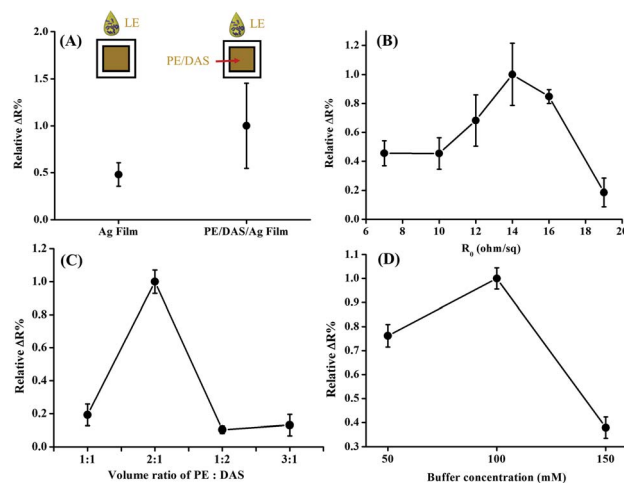


Fig. 1 (A) The relative resistivity changes of the silver film (Ag film) and PE/DAS/Ag film ($N = 3$). The different coating test is also illustrated in (A). The relative resistivity change of (B) PE/DAS/Ag film against LE ($N = 9$), (C) different molar ratio of PE *versus* DAS ($N = 3$), and (D) buffer concentrations at pH 7 ($N = 3$).



resistivity changes were compared. The best response was obtained at a ratio of 2 : 1. We surmised that PE in higher concentrations would react with LE and force the reaction to proceed according to the Le Chatelier principle. However, increases in PE would produce more products and then drive the reaction to the left, further decreasing the resistivity change.

As seen in Fig. 1(D), the resistivity changes of various concentrations of buffer were compared. The buffer concentration was varied from 50 to 150 mM, and LE (or DAS) was dissolved to the same buffer concentration. It was found that the resistivity change decreased with increasing buffer concentration or ionic strength, suggesting that the higher ionic strength limited the enzyme's activity and further decreased the formation of products. The maximum resistivity change and the smallest deviation between the results were obtained at 100 mM. Thus, the buffer concentration of 100 mM was considered optimum.

Sensing mechanism of the LE-PAD device

SEM images of LE-PADs are shown in Fig. 2. In that figure, spherical particles with wires are visible among the cellulose fibres of the paper in the response region of an LE-PAD with Ag film only (Fig. 1(A) and (B)). The EDS spectrum of this region showed clear peaks of carbon, nitrogen, oxygen and silver, indicating that the Ag film consisted of silver nanoparticles and silver nanowires (Fig. S1(A)† and 2(B)). Comparison of the contact angles of the silver ink (Ag ink surface) and the Ag film

(Fig. S2(A) and (B)†) showed that the contact angle increased from 5.7° to 32.7°; this change indicated that the silver coating was transformed from hydrophilic to more hydrophobic after light sintering.

Upon addition of LE to the sample inlet region (PE/DAS/Ag film), the UV spectrum at the response region was exploited. The emergence of a new absorption band at 580–650 nm and the purple colour both indicated azo compound formation (Fig. S3†). Furthermore, SEM images and EDS analysis of samples without and with LE added, namely, PE/DAS/Ag film and LE/PE/DAS/Ag film, respectively, were used to compare changes in morphology (Fig. 2(D), (F) and S1(A), (B)†). The morphologies of the response region of samples without and with LE added were obviously different. In the presence of LE, the diameters of the nanospheres in Fig. 2(D) increased from 67–83 nm to 83–150 nm, as shown in Fig. 2(F). In addition, the amount of nanospheres decreased and some nanosticks formed. Simultaneously, the relative contents of carbon and nitrogen increased and that of oxygen slightly decreased by more than 5% with LE added, as demonstrated by the energy spectrum of a sample without LE (Fig. S1(A)†), which indicated that the amount of the organic component, *i.e.*, azo compound, increased in the response region.

The FTIR spectra related to each studied compound are displayed in Fig. S4.† Characteristic PE bands in Fig. S4(A)† would be at $\sim 3377\text{--}3344\text{ cm}^{-1}$, related to stretching vibration of N–H groups; at $\sim 1349\text{--}1322\text{ cm}^{-1}$, due to S=O stretching vibration of sulfonamide groups. The band at 1764 cm^{-1} would be due to stretching vibration of carbonyl groups. There is an absorption weak band at 3033 cm^{-1} that is assigned to C–H vibration of aromatic rings.³⁰ The IR spectrum of DAS (Fig. S4(B)†) showed that IR absorption peaks at 3253 and 3082 cm^{-1} that were assigned to O–H and C–H stretching, respectively. Vibration peaks observed at $1615\text{--}1568\text{ cm}^{-1}$ were attributed to N=N stretching. The absorption bands exhibited at 1511 and 1440 cm^{-1} which are assigned to C=C stretching. The asymmetry stretching vibration of S–O (–SO₃H) group appearance at 1144 and 1054 cm^{-1} . In addition, C–H asymmetric peak was appeared at $1239\text{--}1208\text{ cm}^{-1}$.³¹ As can be seen in Fig. S4(C),† there is a peak at 2923 and 1436 cm^{-1} ascribed to asymmetric stretching vibration of CH₂ of PVP group. The peaks at 1643 and 3428 cm^{-1} conform the –C=O and –OH of PVP capped Ag film. The appearance of deep absorption band at 1290 cm^{-1} that was assigned to C–N vibration.³² The FTIR spectra of the coating on the LE-PAD device are shown in Fig. 3. When we compared the FTIR spectra of the control samples, *i.e.*, PE/DAS and LE/PE/DAS, and that of LE/PE/DAS/Ag film, differences in some peaks were noticed. The peak positions of LE/PE/DAS at wavenumbers of 3320–3380, ~ 3240 , 2079, 2225, and 1611 cm^{-1} were ascribed to N–H stretching, –OH stretch, –C–C=C–C=CH, [†]R–N=N (diazonium), and R–N=N–R (azo),³³ respectively, indicating azo product formation on the paper device (Fig. 3(A) and (B)). The FTIR spectrum of the LE/PE/DAS/Ag film had similar peak positions, supporting the formation of azo product on the silver film (Fig. 3(C)). In particular, comparing Fig. 3(B) and (C) shows that these peaks did not shift much to support the hydrogen bond formation

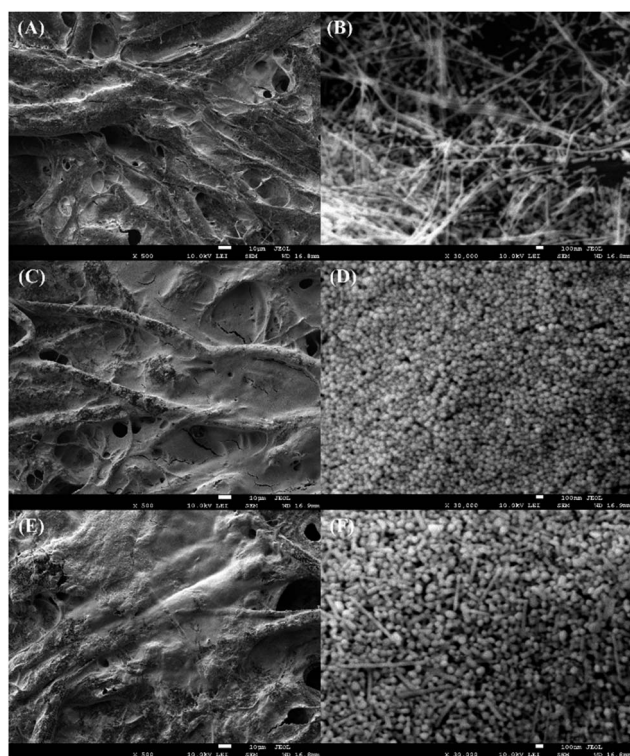


Fig. 2 SEM images: (A and B) Ag film, (C and D) PE/DAS/Ag film and (E and F) LE/PE/DAS/Ag film. The scale bars are 10 μm (A, C and E) and 100 nm (B, D and F).



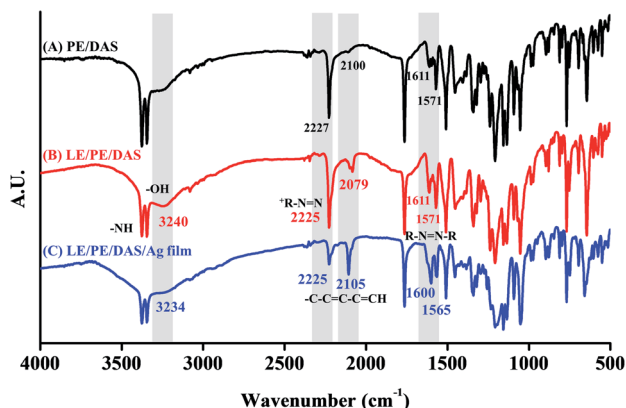


Fig. 3 IR spectra of PE/DAS (A), LE/PE/DAS (B), LE/PE/DAS/Ag film (C) on LE-PADs.

between compounds and silver coating. In addition, it was noticed that the decrease in the absorption band around 2225 cm^{-1} accompanied by the increase at 1600 cm^{-1} of the LE/PE/DAS/Ag film indicated that the silver coating facilitated the formation of the azo compound on the paper-based device.

Quantification of LE and linear regression

The change in resistivity on detection of LE was measured using LE-PADs in optimum conditions. The calibration curve for LE is shown in Fig. 4. It was found that the resistivity change increased linearly with increases in LE concentration. The linear segment was in the range of 2.0 to 8.0 ($\times 5.1\text{ U mg}^{-1}\text{ mL}^{-1}$). The calibration equation obtained was $\Delta R\% = 0.087[\text{LE}] + 0.238$ ($R^2 = 0.9908$). From the results of SEM-EDS analysis, absorption spectra, and FTIR spectra of samples without and with LE added, an azo compound, *i.e.* a non-conductive material, which was produced onto Ag film after LE was reacted with PE and DAS. Thus, we can deduce the reaction mechanism of

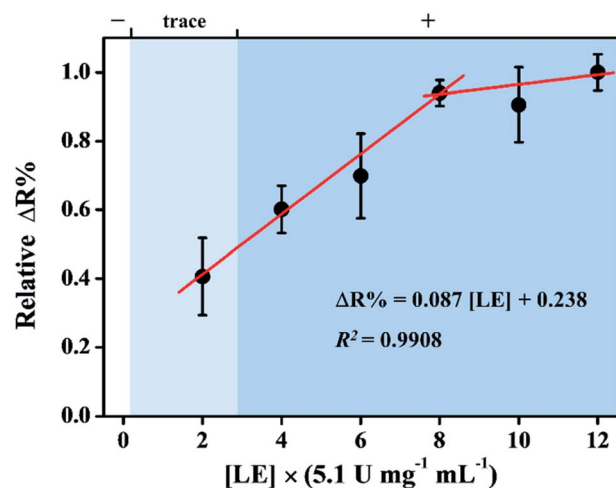


Fig. 4 The relative resistivity change of LE-PADs as a function of the LE. The SD of three independent experiments. The diagnosis zone of UTI from commercial colorimetric test strips is also presented in the figure.

LE-PADs with LE. The LE/urine reacts with the PE and DAS, and the resulting products, *e.g.* a non-conductive azo product, in turn deposition onto the silver coating, causing a resistivity increase in the linear concentration region. The detection limit was deduced to be 1.91 ($\times 5.1\text{ U mg}^{-1}\text{ mL}^{-1}$, $S/N = 3$). The results of different concentrations of LE measured by the commercial colorimetric test strips are also presented in Fig. 4. The relative resistivity of background (buffer only) is 0.29 ($\Delta R\%$). To the best of our knowledge, the applications of electrochemical method to the determination of LE in urine are very rare. There are two reports published from Gorski group.^{17,18} Compared with the amperometric measurement,¹⁷ at which the lowest limit of detection of LE is around 1.92 ($\times 5.1\text{ U mg}^{-1}\text{ mL}^{-1}$; $20\text{ WBC per } \mu\text{L}$), the LE-PADs possesses a similar detection limit.

Interference study

To discover the influence of potential interferences in human urine, the most abundant constituents of urine in healthy individuals were studied. The list of average constituent concentrations in human urine is shown in Table S1.† The concentration of these constituents were 10 – 10^6 folds larger than their average constituent concentrations in healthy body. When we used the real urine test (see Fig. 5), *i.e.* control signal, the relative resistivity change of healthy individual urine which contains all of the potential interferes is 0.06 ($\Delta R\%$). Accordingly, other species in urine did not cause significant interference in this assay. Furthermore, based on the calibration curve, after addition of 2.0 ($\times 5.1\text{ U mg}^{-1}\text{ mL}^{-1}$) LE to the urine sample, the relative intensity change is 0.41 ($\Delta R\%$). In clinical diagnosis, 2.0 ($\times 5.1\text{ U mg}^{-1}\text{ mL}^{-1}$) LE is response to the “trace” zone of commercial colorimetric test strips (Fig. 4). The relative

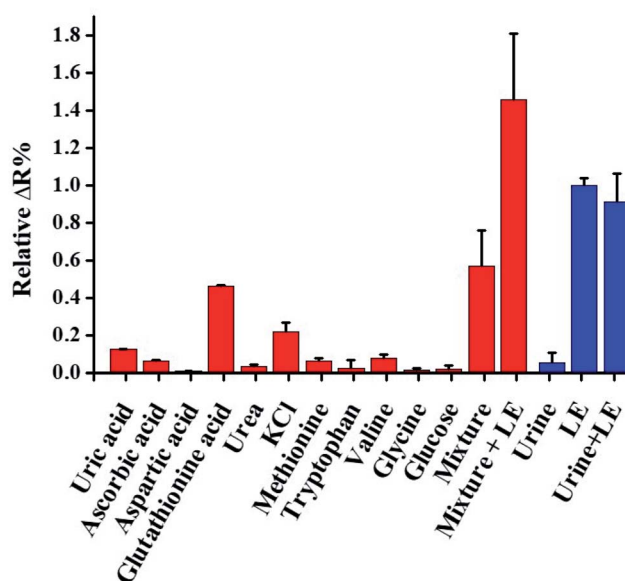


Fig. 5 Selectivity of the LE-PADs against other potential interferent species in urine. The mixture (10 mM) means the coexistence of all interferents ($N = 3$).



resistance change increased by approximately 6.8-fold upon 2.0 ($\times 5.1 \text{ U mg}^{-1} \text{ mL}^{-1}$) LE addition; hence, the device can be used to quantify LE in urine. When this potential interferes were added to the LE-PADs, the relative resistivity change was analysed in triplicate. The effects of the mixture of these constituents and human urine without dilution or any pre-treatment procedures against 8.0 ($\times 5.1 \text{ U mg}^{-1} \text{ mL}^{-1}$) LE were evaluated. The relative resistivity changes (Fig. 5) indicated good selectivity of the LE-PADs toward LE.

The storage stability

The storage stability of the LE-PADs was examined for 2 months in 8.0 ($\times 5.1 \text{ U mg}^{-1} \text{ mL}^{-1}$) LE. As shown in Fig. S4,† the relative resistivity change of the LE-PADs remained stable, with 95.4% resistivity change within two months, which implies that the LE-PADs could be stored for at least two months.

Real samples analysis

Collected from 16 patients with indwelling urinary catheters with suspected UTIs, 8 urine samples with compatible UTI findings required for clinical diagnosis and 13 without were tested by LE-PADs. According to clinical data, all of the 8 urine samples were culture-positive for bacteria or fungus and demonstrated pyuria with >10 leukocyte per high power field (HPF) based on microscopic examination.³⁴ (see ESI Table S2† for detailed information).

Using dipsticks, among 21 urine samples, 8 tested positive for LE: 5 (62.5%) in 8 UTI samples and 3 (23.1%) in 13 non-UTI samples ($p = 0.012$). However, only 4 urine samples tested positive for nitrite by dipsticks: 4 (50.0%) in 8 UTI samples and none in 13 non-UTI samples ($p = 0.164$). Here, the sensitivity and specificity of dipstick LE positivity on diagnosing UTI were 62.5% (5/8) and 76.9% (11/13), respectively. When dipstick LE and/or nitrite positivity were used to detect UTI, the sensitivity increased to 87.5% (7/8) and specificity remained at 76.9% (11/13) (Table 1).

Using the LE-PAD, the median LE level of the 21 urine samples was 4.61 ($\times 5.1 \text{ U mg}^{-1} \text{ mL}^{-1}$) [IQR 2.39–7.78, a level of >8.00 was treated as 8.00]. The median LE level was 7.96 ($\times 5.1 \text{ U mg}^{-1} \text{ mL}^{-1}$) [IQR 7.73–8.00] in UTI urine samples and 4.37 ($\times 5.1 \text{ U mg}^{-1} \text{ mL}^{-1}$) [IQR 2.21–6.99] in non-UTI urine samples ($p = 0.003$). In a receiver operating characteristic (ROC) curve analysis, the optimal cut-off point for discriminating UTI was 7.60 ($\times 5.1 \text{ U mg}^{-1} \text{ mL}^{-1}$), and the area under the ROC was 0.875 (95% CI, 0.704–1.000). Based on this cut-off point, 8 urine samples had high LE-PAD levels: 7 (87.5%) in 8 UTI samples and

1 (8.0%) in 13 non-UTI samples ($p = 0.001$) (also see Tables S2 and S3†). As shown in Table 1, the sensitivity and specificity of LE-PADs on diagnosing UTI were 87.5% (7 of 8 UTI samples were tested positive) and 92.3% (12 of 13 non-UTI samples were tested negative) (also see Table S3†). Notably, the positive and negative likelihood ratios were 11.38 and 0.14, respectively. Considering the 4 parameters, including sensitivity, specificity, positive predictive value, and negative predictive value, the performance of the LE-PAD for UTI diagnosis was better than that of dipstick LE. In addition, because the positive likelihood ratio was >10 and the negative likelihood ratio was near 0.1, the LE-PAD should be a reliable test (Table 1).

Conclusions

In this work, a chemiresistive LE sensor manufactured on paper substrate is presented. The LE-PAD provides quantitative determination of LE activity in human urine and thus may facilitate the early detection of UTI. The design has advantages over the common colorimetric assay for quantitative determination of LE using microliter urine without any pre-treatment procedures. Clinical urine samples were used to assess the practical performance of the LE-PAD for UTI diagnosis. Importantly, the LE-PAD had higher sensitivity and specificity than those of dipstick LE and demonstrated positive and negative likelihood ratios of 11.38 and 0.14, suggesting that it is a reliable clinical test.

Experimental sections

Material and reagents

Acetonitrile was acquired from Acros Organic. 3-(*N*-Tosyl-L-alaninyloxy)-5-phenylpyrrole (PE) was obtained from Angene. 1-Diazo-2-naphthol-4-sulfonic (DAS) was from Tokyo Chemical Industry Co., Ltd. Leukocyte Esterase (LE) was from MyBio-Source. Sodium dihydrogen phosphate and disodium hydrogen phosphate were from Merck. Ethylene glycol (EG) and sodium chloride were from J. T. Baker. Silver nitrate, polyvinylpyrrolidone (PVP), ethanol (EtOH), D-glucose, ascorbic acid, urea, uric acid, L-tryptophan, L-valine, L-methionine, glycine, L-aspartic acid free acid, potassium chloride, and glutathione acid were from Sigma-Aldrich. Quantitative filter paper no. 5C was acquired from Toyo Roshi Kaisha, Ltd. PBS buffer solution was prepared by mixing with NaH_2PO_4 and Na_2HPO_4 in deionized water.

Table 1 Analysis of dipsticks parameters and experimental measurement with 95% confidence intervals (CI)^a

	Sensitivity, %	Specificity, %	Positive likelihood ratio	Negative likelihood ratio
LE dipstick positivity	62.5 (24.5–91.5)	76.9 (46.2–95.0)	2.71 (0.88 to 8.37)	0.49 (0.19 to 1.25)
Nitrite dipstick positivity	50.0 (15.7–84.3)	100.0 (75.3–100.0)	—	0.50 (0.25–1.00)
LE and/or nitrite dipstick	87.5 (47.4–99.7)	76.9 (46.2–95.0)	3.79 (1.36 to 10.58)	0.16 (0.03 to 1.04)
LE-PAD cut-off positivity	87.5 (47.4–99.7)	92.3 (64.0–99.8)	11.38 (1.70–76.15)	0.14 (0.02–0.85)

^a LE indicates leukocyte esterase; PAD, paper-based analytical device.



LE-PADs fabrication

LE-PADs was printed on Advantec filter paper (no. 5C) using a wax printer (XEROX ColorQube 8880, Norwalk, USA). The printed pattern was then baked at 60 °C for 1 min, thereby allowing the wax to penetrate the back of the filter paper. The pattern was designed as shown in Scheme 1.

Preparation of the silver nanoparticles (AgNPs) and silver film (Ag film)

Silver nanoparticles (AgNPs) were synthesized through a polyol process, in which PVP acts as a capping agent, EG works as both a reducing reagent and solvent, and NaCl acts as seed crystals to facilitate the production of silver nanowires.³⁵ Details of the synthesis procedure of AgNPs have been previously described elsewhere.²⁶ At first, NaCl (30 mM) was added to 30.2 mL EG solution of AgNO₃ (50 mM) and PVP (280 mM) at a flow rate 1.0 mL min⁻¹. Then, the mixture was refluxed at 130 °C for 30 min. After these processes, the excess PVP and EG were removed by adding ethanol centrifuged at 12 000 rpm for 20 min at room temperature. After centrifugation, the supernatant was removed and the formed AgNPs were left at the bottom. In the next step, the solvent composition of silver ink was water : ethanol = 5 : 95 vol%. AgNPs was added into this solvent. The resulting silver ink was dispersed by ultrasonic treatment and then used to prepare flexible silver film (Ag film).

A conductive Ag film was prepared by dropping 6 µL AgNP ink on the surface of the response region of the LE-PAD, followed by intensive pulsed light sintering to achieve high conductivity.

Sintering of AgNPs ink by intensive pulse light

Intensive pulsed light (MPL 1515S) was generated from a xenon flash lamp. The distance between the lamp and the film was 5.0 cm. The sintering condition was fixed at 1 s, 4 pulses and 1.64 J cm⁻². The electrical resistivity of the resulting silver film (R_0) was measured by four-point probe station (Keithley 2000-EM4P) and was calculated from sheet resistance and film thickness. The four-point probe station can also be replaced with a portable four-point probe.

Preparation of LE-PADs and the determination of optimized conditions of LE-PADs

To optimize the conditions of the LE-PADs, 10 mg mL⁻¹ PE was dissolved in acetonitrile and 5 mg mL⁻¹ DAS was dissolved in PBS buffer solution at pH 7.0. 10 µL of mixture solution of PE and DAS was added to the silver coating, followed by drying at room temperature for 5 min. Optimized LE-PADs were tested for resistivity changes by adding a Stock solution of LE (8 × 5.1 U mg⁻¹ mL⁻¹). The concentrations of PBS buffer (50, 100 and 150 mM) was tested first. Subsequently, different molar ratios of the PE-DAS solution (PE : DAS = 1 : 1, 2 : 1, 1 : 2 and 3 : 1) were optimized.

Characterization

The morphologies, microstructural evolution and elemental composition of the silver film were investigated using field-emission scanning electron microscopy (FE-SEM) coupled with energy dispersive X-ray spectroscopy (EDX, JEOL JSM-7600F). Furthermore, the optical absorbance and transmittance spectra were measured using a UV-visible-near IR spectrophotometer (Hitachi U-4100). The contact angle of the silver film on paper was surveyed by the sessile drop technique (KRÜSS DSA100S).

Detection of LE

Stock solutions of LE (2.0–8.0 × 5.1 U mg⁻¹ mL⁻¹) were prepared by dissolving different volumes of LE in 1 mL PBS buffer solution at pH 7.0. The procedure of analyte detection (LE stock solution in PBS buffer at pH 7.0 or human urine with any pre-treatment steps) on the LE-PADs involved the addition of 10 µL of analyte solution onto the LE-PADs device. The sheet resistance change after LE addition was determined by eqn (1). R_0 was the initial sheet resistance, and R_1 was the sheet resistance measured after LE or human urine addition, respectively.

$$\Delta R\% = \frac{R_1 - R_0}{R_0} \times 100\% \quad (1)$$

Interference effect

To investigate the effect of the potential interferents, the most abundant constituents of urine were collected from a healthy individual, including D-glucose, ascorbic acid, urea, uric acid, L-tryptophan, L-valine, L-methionine, glycine, L-aspartic acid free acid, potassium chloride, and glutathione acid. The interferents were mixed in PBS buffer solution, and human urine from a healthy male (age 21) were measured for LE.

The storage

The stability of the LE-PADs was evaluated by adding 8.0 (× 5.1 U mg⁻¹ mL⁻¹) LE to the LE-PADs. During the storage period, LE-PADs were stored at room temperature in a zip-lock bag containing a desiccant, both purchased on the local market.

Clinical human urine for detection by the LE-PADs

The clinical study protocol including the process of urine sample collection in human subjects was approved by the institutional review board of Taipei Veterans General Hospital in Taiwan (No. 2018-05-006CC). Informed consent was obtained from all human subjects and all experiments were performed in accordance with the Declaration of Helsinki Ethical Principles. The urine samples were prospectively collected from inpatients with an indwelling urinary catheter (IUC) in place at the respiratory care centre (RCC), a subacute care ward for mechanically ventilated patients in this hospital. The most common indication of IUC use in RCC patients was acute urinary retention, followed by urine amount monitoring in rare clinical conditions. From September 2018 to January 2019, adult RCC



patients were consecutively screened for IUC use and suspected UTI.

As a clinical routine at RCC, in IUC patients with a clinically suspected UTI, urine samples are collected for examination through aseptic procedure. The samples are processed by the routine urinalysis, consisting of a chemical examination including LE and nitrite using chemical test strips.³⁶ In addition, urine microscopic examinations are also performed on centrifuged catheter urine specimens to identify red blood cells, leukocytes, bacteria, and others. The urine culture, if indicated, is also performed according to the clinical order.

For the study measurement, for enrolled IUC patients with suspected UTI, a 20cc urine sample was collected within one day through the puncture of the IUC tubing with a needle *via* sterile technique.³⁷ If an enrolled patient did not have a UTI diagnosis, as second measurement, an additional 20cc urine from the same patient, was collected again if he or she still had the IUC in place one week later. In contrast, if a patient had a UTI diagnosis and received antibiotic treatment, no second test was done. All urine samples were stored at 4 °C and tested within 4 hours for study purpose. The urine was applied to the LE-PADs to detect the presence of LE. 10 µL of urine without any pre-treatment was added to the LE-PADs. The resistivity before and after the addition of urine were recorded, and the change in resistivity was calculated.

The diagnosis of UTI was made by a clinical physician if (1) a patient had fever or urinary tract symptoms with leucocytosis, (2) there was positive urinalysis with pyuria (urine leukocyte ≥ 10 per HPF) with bacteriuria, and (3) positive urine culture (with a bacterial count of $\geq 10^3$ colony forming units per mL of urine specimen).³⁴ The characteristics and diagnosis of UTI were recorded on the medical charts of the patients. Finally, the sensitivity and specificity of dipstick LE, nitrite and our study measurement to detect UTI were assessed.

Statistical analysis

Continuous data are presented as median with interquartile range (IQR) for preventing “skewness” in statistical analysis. The median takes into account only the number of cases above and below the median point, not the value of these cases.³⁸ So the value will not be affected in any way if more of the data values are clustered toward one end of their range and/or if there are a few extreme values.³⁸ The differences between groups are examined by Mann–Whitney *U* tests. Individual LE levels were used to perform all the statistics. Dichotomous variables are shown as *n* (%), and χ^2 test was used as appropriate. For the measurement setup, a linear regression model was also used to assess the associations between the relative resistivity change of LE-PADs and the levels of LE; *R*-square was calculated as a goodness-of-fit measure. For clinical application, receiver operating characteristic curve analysis and the Youden index were used to investigate the optimal cut-off point of measurement by LE-PAD. Using the cut-off point, the sensitivity and specificity of the LE-PAD for UTI diagnosis were calculated and compared with those of dipstick LE. Additionally, the positive and negative likelihood ratios of diagnostic tests were

calculated. Regarding the performance measurement of the tests, a positive likelihood ratio of > 10 and a negative likelihood ratio of < 0.1 were considered as reliable. SPSS software (version 18.0) was used for statistical analyses.

Conflicts of interest

There are no conflicts to declare.

Acknowledgements

This work was supported by the Ministry of Science and Technology, Taiwan. The authors are grateful to Ms S.-J. Ji of the Ministry of Science and Technology (National Taiwan University) for her assistance in the SEM/EDS experiments.

References

- 1 A. L. Flores-Mireles, J. N. Walker, M. Caparon and S. J. Hultgren, *Nat. Rev. Microbiol.*, 2015, **13**, 269–284.
- 2 J. B. L. Lee and G. H. Neild, *Medicine*, 2007, **35**, 423–428.
- 3 A. Masajtis-Zagajewska and M. Nowicki, *Clin. Chim. Acta*, 2017, **471**, 286–291.
- 4 B. Foxman, *Am. J. Med.*, 2002, **113**, 5–13.
- 5 M. Fritzenwanker, C. Imirzalioglu, T. Chakraborty and F. M. Wagenlehner, *Expert Rev. Anti-Infect. Ther.*, 2016, **14**, 1047–1063.
- 6 A. S. Kupelian, H. Horsley, R. Khasriya, R. T. Amussah, R. Badiani, A. M. Courtney, N. S. Chandhyoke, U. Riaz, K. Savlani, M. Moledina, S. Montes, D. O'Connor, R. Visavadia, M. Kelsey, J. L. Rohn and J. Malone-Lee, *BJU Int.*, 2013, **112**, 231–238.
- 7 P. Mejuto, M. Luengo and J. Díaz-Gigante, *Internet J. Microbiol.*, 2017, **2017**, 1–8.
- 8 M. Davenport, K. E. Mach, L. M. D. Shortliffe, N. Banaei, T. H. Wang and J. C. Liao, *Nat. Rev. Urol.*, 2017, **14**, 296–310.
- 9 Y. Zboromyrska, E. Rubio, I. Alejo, A. Vergara, A. Mons, I. Campo, J. Bosch, F. Marco and J. Vila, *Clin. Microbiol. Infect.*, 2016, **22**, 561.
- 10 B. Shadgan, M. Nigro, A. Macnab, M. Fareghi, L. Stothers, L. Sharifi-Rad and A.-M. Kajbafzadeh, *J. Pediatr. Neurol.*, 2015, **11**, 74.
- 11 K. B. Barken, J. A. J. Haagensen and T. Tolker-Nielsen, *Clin. Chim. Acta*, 2007, **384**, 1–11.
- 12 G. Bonkat, O. Braissant, M. Rieken, A. Solokhina, A. F. Widmer, R. Frei, A. van der Merwe, S. Wyler, T. C. Gasser and A. Bachmann, *World J. Urol.*, 2013, **31**, 553–557.
- 13 P. Béland, O. Krupin and P. Berini, *Biomed. Opt. Express*, 2015, **6**, 2908–2922.
- 14 J. Parvizi, C. Jacovides, V. Antoci and E. Ghanem, *J. Bone Jt. Surg., Am. Vol.*, 2011, **93**, 2242–2248.
- 15 R. Li, X. Li, B. Yu, X. Li, X. Song, H. Li, C. Xu and J. Chen, *Med. Sci. Monit.*, 2017, **23**, 4440–4446.
- 16 T. Sapey, E. Mena, E. Fort, C. Laurin, D. Kabissa, B. A. Runyon and M.-H. Mendler, *J. Gastroenterol. Hepatol.*, 2005, **20**, 187–192.



- 17 D. Hanson, T. Menard, T. Blazek, S. McHardy and W. Gorski, *ChemBioChem*, 2018, **19**, 1488–1491.
- 18 D. Hanson, T. Menard, S. McHardy, A. Fleischman and W. Gorski, *Anal. Chem.*, 2017, **89**, 7781–7787.
- 19 M. L. Sin, K. E. Mach, P. K. Wong and J. L. Liao, *Expert Rev. Mol. Diagn.*, 2014, **14**, 225–244.
- 20 K. Rajan, I. Roppolo, A. Chiappone, S. Bocchini, D. Perrone and A. Chiolerio, *Nanotechnol., Sci. Appl.*, 2016, **9**, 1–13.
- 21 S. Merilampi, T. Björninen, V. Haukka, P. Ruuskanen, L. Ukkonen and L. Sydänheimo, *Microelectron. Reliab.*, 2010, **50**, 2001–2011.
- 22 H. Andersson, A. Manuilskiy, T. Unander, C. Lidenmark, S. Forsberg and H.-E. Nilsson, *IEEE Sens. J.*, 2012, **12**, 1901–1905.
- 23 H. Andersson, A. Manuilskiy, J. Gao, C. Lidenmark, J. Sidén, S. Forsberg, T. Unander and H.-E. Nilsson, *IEEE Sens. J.*, 2014, **14**, 623–628.
- 24 S. Kim, A. Georgiadis and M. M. Tentzeris, *Sensors*, 2018, **8**, 1958–1968.
- 25 M. Labib, E. H. Sargent and S. O. Kelley, *Chem. Rev.*, 2016, **116**, 9001–9090.
- 26 Y.-C. Liu, C.-H. Hsu, B.-J. Lu, P.-Y. Lin and M.-L. Ho, *Dalton Trans.*, 2018, **47**, 14799–14807.
- 27 A. K. Mambatta, J. Jayarajan, V. L. Rashme, S. Harini, S. Menon and J. Kuppusamy, *J. Family Med. Prim. Care*, 2015, **4**, 265–268.
- 28 D. S. Schwartz and J. O. E. Barone, *Intensive Care Med.*, 2006, **32**, 1797–1801.
- 29 M. Bland, *An introduction to medical statistics*, Oxford University Press, Oxford, 2nd edn, 1995, pp. 125–126.
- 30 Y. Chen and W. Hua, *Spectrochim. Acta, Part A*, 2000, **56**, 447–451.
- 31 C. V. Turcaş and I. Sebe, *Sci. Bull. - Univ. "Politeh." Bucharest, Ser. B*, 2012, **74**, 109–118.
- 32 K. M. Koczur, S. Mourdikoudis, L. Polavarapu and S. E. Skrabalak, *Dalton Trans.*, 2015, **44**, 17883–17905.
- 33 L. D. S. Yadav, *Organic Spectroscopy*, Springer, Berlin, 2004.
- 34 T. M. Hooton, S. F. Bradley, D. D. Cardenas, R. Colgan, S. E. Geerlings, J. C. Rice, S. Saint, A. J. Schaeffer, P. A. Tambayh, P. Tenke and L. E. Nicolle, *Clin. Infect. Dis.*, 2010, **50**, 625–663.
- 35 N. V. Nghia, N. N. K. Truong, N. M. Thong and N. P. Hung, *Int. J. Mater. Chem.*, 2012, **2**, 75–78.
- 36 J. A. Simerville, W. C. Maxted and J. J. Pahira, *Am. Fam. Physician*, 2005, **71**, 1153–1162.
- 37 L. E. Nicolle, *Antimicrob. Resist. Infect. Control*, 2014, **3**, 23–30.
- 38 R. D. Bachman and R. K. Schutt, *The Practice of Research in Criminology and Criminal Justice*, SAGE, New York, 2007.

